

## A compact bipolar pulse-forming network-Marx generator based on pulse transformers

Huibo Zhang, Jianhua Yang, Jiajin Lin, and Xiao Yang

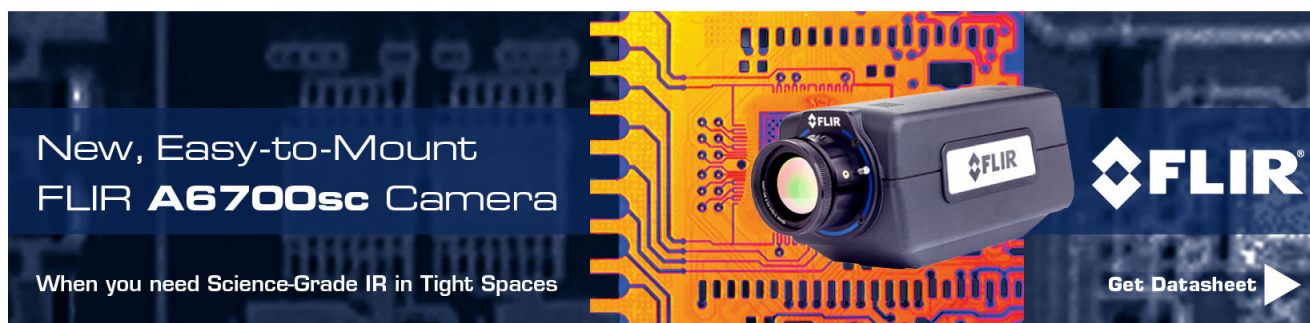
Citation: [Review of Scientific Instruments](#) **84**, 114705 (2013); doi: 10.1063/1.4828793

View online: <http://dx.doi.org/10.1063/1.4828793>

View Table of Contents: <http://scitation.aip.org/content/aip/journal/rsi/84/11?ver=pdfcov>

Published by the [AIP Publishing](#)

---

An advertisement for the FLIR A6700sc camera. The background is a dark blue circuit board with orange and yellow traces. A black FLIR camera module is shown in the center, with its lens and FLIR logo visible. To the left of the camera, the text 'New, Easy-to-Mount FLIR A6700sc Camera' is written in white. Below this, the text 'When you need Science-Grade IR in Tight Spaces' is written in white. To the right of the camera, the FLIR logo is displayed in white. At the bottom right, the text 'Get Datasheet' is written in white, followed by a white right-pointing arrow.

# A compact bipolar pulse-forming network-Marx generator based on pulse transformers

Huibo Zhang,<sup>a)</sup> Jianhua Yang, Jiajin Lin, and Xiao Yang

*College of Optoelectronic Science and Engineering, National University of Defense Technology, Changsha 410073, China*

(Received 24 July 2013; accepted 22 October 2013; published online 8 November 2013)

A compact bipolar pulse-forming network (PFN)-Marx generator based on pulse transformers is presented in this paper. The high-voltage generator consisted of two sets of pulse transformers, 6 stages of PFNs with ceramic capacitors, a switch unit, and a matched load. The design is characterized by the bipolar pulse charging scheme and the compact structure of the PFN-Marx. The scheme of bipolar charging by pulse transformers increased the withstand voltage of the ceramic capacitors in the PFNs and decreased the number of the gas gap switches. The compact structure of the PFN-Marx was aimed at reducing the parasitic inductance in the generator. When the charging voltage on the PFNs was 35 kV, the matched resistive load of 48  $\Omega$  could deliver a high-voltage pulse with an amplitude of 100 kV. The full width at half maximum of the load pulse was 173 ns, and its rise time was less than 15 ns. © 2013 AIP Publishing LLC. [<http://dx.doi.org/10.1063/1.4828793>]

## I. INTRODUCTION

High-voltage square pulses are of great importance for producing long-pulse electron beams and high-power microwaves.<sup>1–3</sup> A pulse forming line (PFL) with a Marx generator or transformer is a common technology for the generation of high-voltage square pulse with pulse durations of a hundred nanoseconds and amplitude of several hundreds of kV.<sup>4–8</sup> However, if a pulse width greater than 200 ns is required, a spiral PFL structure should be employed, which can lead to a complicated PFL system. The dispersion of the spiral PFL can also lead to inferior flat tops of the formed pulses.<sup>5,6,9,10</sup> Additionally, some subsidiary equipment such as a water cycling system is needed especially in the PFL system with a dielectric of deionized water, making the PFL system have a large volume.

A pulse-forming network (PFN), formed by identical inductors and capacitors, has the natural advantage of square pulse generation due to its circuit topology, and the generated pulse width can range from hundreds of nanoseconds to tens of microseconds.<sup>11,12</sup> As the output voltage of a single stage PFN is limited by the insulation strength of the capacitors, the PFN-Marx is proposed to generate high voltage square pulse.<sup>13–16</sup> Kekez designed a 32-stage compact PFN-Marx generator with the pulse width of 500 ns and the voltage of 650 kV, and a pulse sharpening technique was utilized to reduce the rise time to a few nanoseconds.<sup>11,13</sup> Phelps designed a high-density compact PFN-Marx modulator, which achieved a matched load voltage higher than 600 kV and the energy of 1.5 kJ per pulse in a cylindrical volume with a 20 in. diameter by 25 in. long.<sup>14</sup>

However, a traditional PFN-Marx uses a DC charge style, which requires the capacitors in the PFN to withstand the DC high voltage. The self-inductance of the capacitor in the PFN-Marx system could not be reduced effectively, and the inductance introduced by the connection wire is also inevitable.<sup>17</sup>

All of these factors cause a rise time greater than tens of nanoseconds without the pulse sharpening technique.

In this paper, a 6-stage bipolar pulse charged PFN-Marx generator based on pulse transformers is proposed. As pulse transformers were employed, the charging time could be shortened dramatically. Thus, the withstand voltage of the PFN could be further increased. The bipolar charging scheme reduced the number of gas gap switches. The effects of the isolating inductors on the charging voltage and the over-voltage on switches were analyzed. It found that, with a reasonable connection type of the isolating inductors, the over-voltage on the switches could increase. High-voltage ceramic capacitors with low self-inductance were employed in the PFN, and a single stage PFN could withstand a DC voltage of 100 kV. The system structure was also designed to be compact, which was helpful to reduce the loop inductance and improve the quality of the output pulse waveform. The experimental results showed that the PFN-Marx could produce a high-voltage pulse with amplitude of 100 kV on a 48  $\Omega$  load. The full width at half maximum of the load voltage pulse was 173 ns, and its rise time was less than 15 ns.

Section II discusses the discharge characteristic of a single stage PFN. The simulation and design of the bipolar 6-stage PFN-Marx are presented in Secs. III and IV. Section V presents the experimental test results of the PFN-Marx and its promising industrial application, and Sec. VI makes a conclusion of this work.

## II. DISCHARGE CHARACTERISTIC OF THE PFN

A PFN is commonly used to generate long square voltage pulse, and it consists of identical capacitors and inductors. For a uniform ladder network with 8 sections of LC units as shown in Fig. 1, L1 to L8 were the inductors and C1 to C8 were the capacitors. R was the matched load resistor. The voltage across the capacitors and the current through the inductors were simulated by PSpice software.

<sup>a)</sup>Email: zhanghuibo206@gmail.com

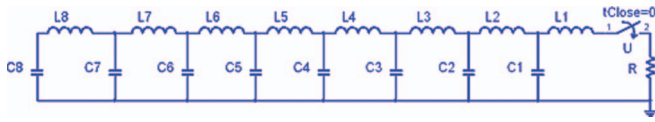


FIG. 1. Equivalent schematic of a PFN with 8 sections of  $LC$  units. ( $L1$  to  $L8$  were the inductors and  $C1$  to  $C8$  were the capacitors.  $R$  was the matched load resistor.)

As shown in Figs. 2(a) and 2(b),  $U_0$  was the initial voltage on each capacitor, and  $I_0$  was maximum current on load resistor. At the beginning of the discharge process, the farther distance the capacitors (inductors) are from the load, the later the voltage (current) on them will change. A capacitor discharged to its former capacitor, such as capacitor  $C2$  discharged to capacitor  $C1$ . At the same time, the capacitor was also charged by the later capacitor, such as capacitor  $C2$  was charged by capacitor  $C3$ . The dynamic equilibrium was that the voltage on a capacitor remained the same (about half of the initial value) until the discharge process of its later capacitor (such as capacitor  $C2$  to capacitor  $C1$ ) was almost over. The discharge process of capacitor  $C8$  finished first. Then, the discharge process finished in turn from capacitor  $C7$  to capacitor  $C1$ .

When  $n$  is large, the pulse generated by the ladder network based on  $n$  sections of  $LC$  units is almost a square waveform. The pulse width,  $\tau$ , characteristic impedance,  $Z$ , and output voltage,  $U$ , on the match load can be expressed as follows:<sup>16</sup>

$$\begin{aligned}\tau &= 2n\sqrt{LC} \\ Z &= \sqrt{\frac{L}{C}} \\ U &= U_0/2,\end{aligned}\quad (1)$$

where  $L$  and  $C$  are the inductance and capacitance of a single section of  $LC$  and  $U_0$  is the initial voltage on the capacitors.

The rise time and fall time of the formed load voltage pulse could be estimated as<sup>18</sup>

$$\begin{aligned}t_r &= 0.8\sqrt{LC} \\ t_f &= 0.8\sqrt{nLC}.\end{aligned}\quad (2)$$

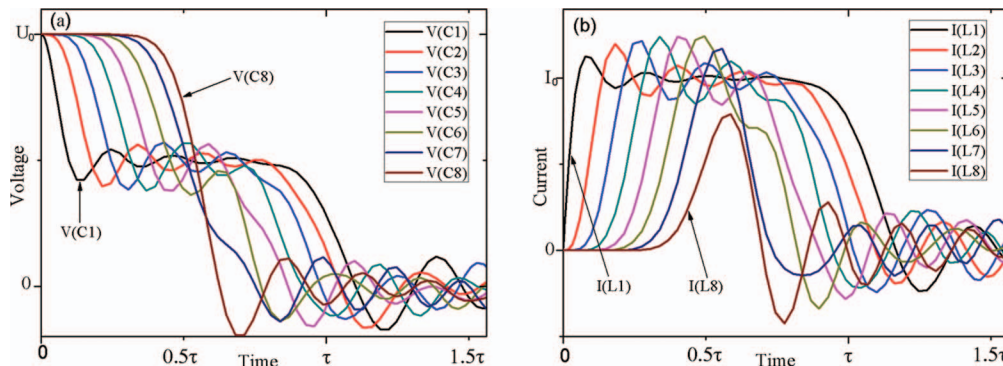


FIG. 2. Voltage on capacitors and current on inductors as functions of discharge time by simulation. (a) Voltage on capacitors vs. discharge time; (b) current on inductors vs. discharge time.  $U_0$  was the initial voltage on each capacitor and  $I_0$  was maximum current on load resistor.

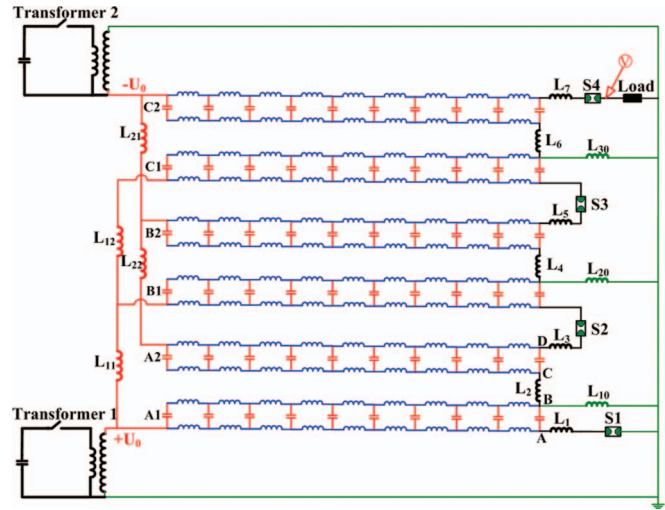


FIG. 3. Equivalent schematic of the 6-stage bipolar PFN-Marx. (This schematic mainly consists of two pulse transformers, four gas gap switches  $S1$  to  $S4$ , 6 stages of PFNs, and the load resistor.)

### III. CIRCUIT SIMULATION OF BIPOLAR PFN-MARX

#### A. The PFN-Marx circuit

The equivalent schematic of a 6-stage bipolar PFN-Marx generator is shown in Fig. 3. This system mainly consisted of two pulse transformers, four gas gap switches, 6 stages of PFNs and the load resistor. The PFNs  $A1$ ,  $B1$ , and  $C1$  were charged by transformer 1 with positive pulse voltage amplitude as  $U_0$ , and the PFNs  $A2$ ,  $B2$ , and  $C2$  were charged by transformer 2 with negative pulse voltage amplitude as  $-U_0$ . The parasitic inductances of the switches and the connection lines were  $L_1$ ,  $L_3$ , and  $L_5$ , respectively. The inductances of the connection line between a pair of PFNs (such as  $A1$  and  $A2$ ) were  $L_2$ ,  $L_4$ , and  $L_6$ . The inductance of the connection lines was in tens of nH, which could be neglected during the charging process. However, it had a strong effect on the rise time of the formed load voltage pulse.  $L_7$  is the inductance of the load loop. The charging inductances were  $L_{11}$ ,  $L_{12}$ ,  $L_{21}$ , and  $L_{22}$ , and the isolating inductances were  $L_{10}$ ,  $L_{20}$ , and  $L_{30}$ . The switches  $S1$ - $S4$ , shown in the circuit, were all self-breakdown gas gap switches.

The operation of the bipolar PFN-Marx generator was as follows: at first, the primary switches of the two



transformers were closed, and the primary capacitors in the transformer discharged to the PFNs. When the charging voltage on the first stage PFN A1 was greater than the voltage that switch S1 could withstand, the gap broke down and the voltage at point A became zero. As the voltage on a capacitor could not change abruptly, the voltage at point B and point D became  $-U_0$  and  $-2U_0$ , respectively, then the voltage across switch S2 became  $3U_0$ . If the breakdown voltage on S2 was set between  $2U_0$  and  $3U_0$ , the gas gap could be broken down. The breakdown of the subsequent switches was similar to the aforementioned case. After all the gas gap switches were closed, the PFN-Marx generator began to discharge through the load. The output voltage on the matched load resistor would be a square pulse.

### B. The uniformity of the charging voltage

Due to the use of bipolar charging pulse transformers in the system, the uniformity of charging voltage on every PFN was investigated. As shown in Fig. 3, the charging inductors  $L_{11}$  and  $L_{12}$  were in a series connection with an inductance of  $100 \mu\text{H}$  each, as were the charging inductors  $L_{21}$  and  $L_{22}$ . The two transformers were same in structure, and were controlled by two sets of different thyristors. The two sets of thyristors could be triggered by a single signal. It could be assumed that the two transformers began to charge to their respective secondary capacitors at the same time. The electromagnetic parameters of the transformer were as follows: the primary capacitance was  $940 \mu\text{F}$ , and the primary and secondary inductances were  $7 \mu\text{H}$  and  $180 \text{mH}$ , respectively. The coupling coefficient is 0.992. Every PFN consisted of 10 sections of  $LC$  units, and the capacitance and inductance of a single section of  $LC$  unit was  $1 \text{nF}$  and  $62 \text{nH}$ , respectively.

In the simulation, it was assumed that the gas gap switches did not break down during the charging process and the withstand voltage of the PFN was high enough. The initial voltage on the primary capacitors was  $500 \text{V}$ . The charging process of the PFN-Marx was analyzed by PSpice software, and the charging voltage waveforms on the PFNs were shown in Fig. 4. It was found that the maximum and minimum charging voltages were  $88.5 \text{kV}$  and  $85.5 \text{kV}$ , respectively, and the relative difference was less than 3%. Therefore, the charging voltage difference on every PFN which was caused by the connective charging inductors could be neglected.

### C. Over-voltage on gas gap switches

The performance of a Marx generator greatly depends on the quality of switches.<sup>19</sup> In order to ensure the stability of the PFN-Marx system, the over-voltage on the switches should be stable and large enough to reduce the jitter of the switches. The over-voltage on every switch was not only depended on the charging voltage, it was also affected by the connection type of isolating inductors. The isolating inductors connected in parallel type and in series type were shown in Figs. 5(a) and 5(b). In fact, the isolating inductors were not connected in exact parallel and series, and here we called them parallel type and series type, respectively. The isolat-

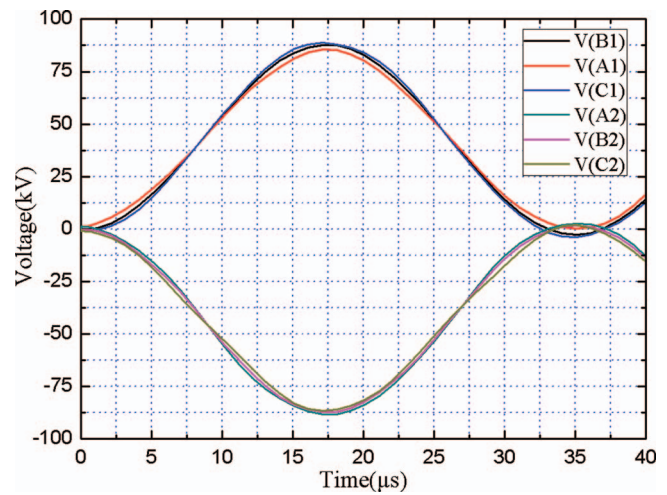


FIG. 4. The charging voltage on every PFN vs. discharge time by simulation. (The PFN A1, B1, and C1 were charged with positive pulse voltage by transformer 1, and the PFN A2, B2, and C2 were charged with negative pulse voltage transformer 2. The initial voltage on the primary capacitors of transformer was  $500 \text{V}$ .)

ing inductors in Fig. 3,  $L_{10}$ ,  $L_{20}$ , and  $L_{30}$ , were connected in parallel type. The over-voltage on every switch with isolating inductors connected in parallel type and series type as analyzed by simulation.

The simulation circuit was similar to the circuit shown in Fig. 3 except for the transformers. Here, we assumed the charging process by the transformers was over and the voltage on every PFN was  $U_0$ . The conducting time of all four spark gap switches was  $5 \text{ns}$ , and they closed at  $t = 0 \text{ns}$ ,  $t = 20 \text{ns}$ ,  $t = 40 \text{ns}$ , and  $t = 60 \text{ns}$ , respectively, which resulted in the load voltage pulse beginning at  $t = 65 \text{ns}$ . As shown in Fig. 6, the over-voltage on every switch with isolating inductors connected in parallel type and in series type was displayed as solid lines and dashed lines, respectively. The over-voltage on S2 with isolating inductors in parallel type connection was almost  $2.5U_0$ , while the over-voltage on S2 with series type connection was only  $2U_0$ . The over-voltage on S3 with parallel type and series type connections were  $4U_0$  and  $2.5U_0$ . The over-voltage on S4 was  $6U_0$  for both connection cases. The over-voltage on S2 and S3 with inductors in parallel type was much higher than the over-voltage on them with inductors in series type connection.

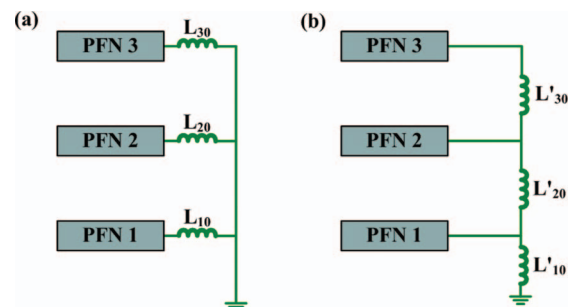


FIG. 5. Isolating inductors between adjacent PFNs with connection in parallel type and in series type. (a) Isolating inductors  $L_{10}$ ,  $L_{20}$ , and  $L_{30}$  were connected in parallel type; (b) isolating inductors connected in series type.

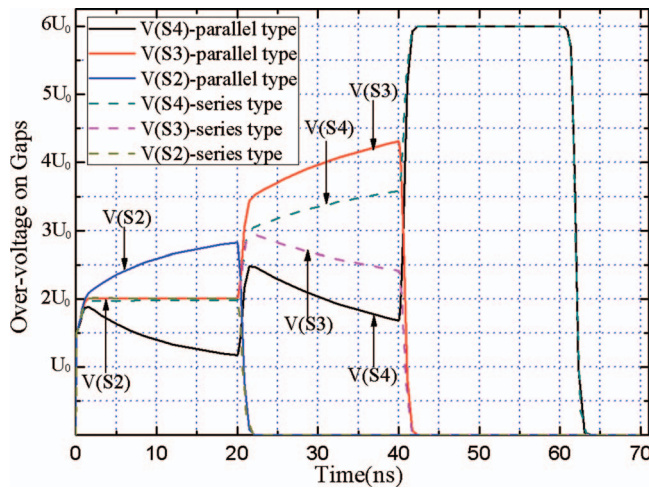


FIG. 6. Over-voltage on switches S2, S3, and S4 by simulation. ( $U_0$  was the initial voltage on every PFN. The conducting time of all four spark gap switches was 5 ns, and they closed at  $t = 0$  ns,  $t = 20$  ns,  $t = 40$  ns, and  $t = 60$  ns, respectively.)

The discharge process was transient, and the isolating inductor can be seen as a large resistance during the process. If all the isolating inductors, such as  $L_{10}$ ,  $L_{20}$ , and  $L_{30}$ , were connected with the ground potential in parallel type connection, as shown in Fig. 3, every stage PFN can be seen as an individual unit. The peak over-voltage on every switch was  $2U_0$ ,  $4U_0$ , and  $6U_0$ , respectively. However, if all the isolating inductors in Fig. 3 were in series type connection, such as  $L'_{10}$ ,  $L'_{20}$ , and  $L'_{30}$ , they were in a circuit loop. The voltage on an isolating inductor could affect the voltage on another isolating inductor. With a certain electrode structure and spacing, the higher over-voltage on a gas switch could lead to a lower jitter of it.<sup>20</sup> Therefore, the parallel type connection of the isolating inductors was chosen in the system.

#### D. Output of the bipolar PFN-Marx in simulation

Some electromagnetic parameters of the 6-stage PFN-Marx were defined as follows. The important electromagnetic parameters of the PFN-Marx were measured using an accurate meter “HP4284A.” Every PFN consisted of 10 sections of  $LC$  units. The capacitance and inductance of a single  $LC$  unit were 1 nF and 62 nH, respectively. It could be calculated by Eq. (1) that the pulse width of a single stage was about 160 ns, and the output voltage on the match load was  $U_0/2$ . The impedance of a single stage PFN was calculated as  $8 \Omega$ , the match impedance of the 6-stage PFN-Marx was  $48 \Omega$ . Other parameters were also shown in Table I.

Based on these parameters, the output characteristic of the PFN-Marx was also investigated by PSpice simulation. As the simulation above, the switch S4 closed a

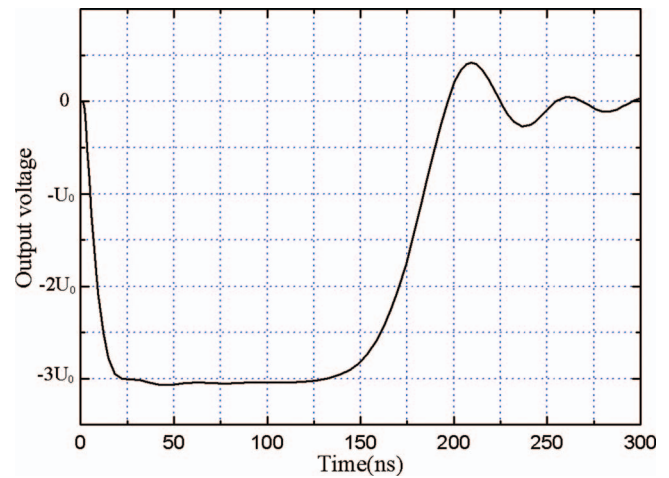


FIG. 7. Output voltage waveform on the load in simulation vs. discharge time by simulation. (The load resistance was  $48 \Omega$ . It was assumed that the load voltage pulse beginning at  $t = 0$  ns.)

$t = 60$  ns, which resulted in the load voltage pulse beginning at  $t = 65$  ns. For simplicity, it was assumed that the load voltage pulse beginning at  $t = 0$  ns. The output voltage waveform on the load with resistance of  $48 \Omega$  was simulated as shown in Fig. 7. It can be seen that the pulse width, defined as full width at half maximum, was about 170 ns, and the output voltage was three times of the charging voltage  $U_0$  on every PFN. The pulse width of 6-stage PFN-Marx corresponded with the theoretical calculation result of a single stage PFN, and the output voltage was six times of the output voltage obtained by a single stage PFN. The PFN-Marx achieved the multiplication of voltage without changing the pulse width of the PFN.

## IV. DESIGN OF 6-STAGE PFN-MARX

### A. Single stage PFN

As we mentioned above, if a PFN-Marx with a fast rise time was required, the loop parasitic inductance which includes the wire connection inductance and the self-inductance of the capacitors must be reduced. The ceramic capacitor with a high relative permittivity and withstand voltage was a promising energy storage unit for compact pulse power devices. Besides, with the development of the fabrication technique of the ceramic capacitor, the self-inductance of the ceramic capacitor has been reduced significantly and the DC voltage that a single cell could withstand has been up to 50 kV.<sup>21,22</sup> Therefore, PFN with ceramic capacitor could generate long high-voltage pulse with rise time of nanoseconds.

The capacitance of a single cell was 2 nF. If two cells were connected in series, the capacitance becomes 1 nF and the voltage it could withstand could be 100 kV. In order to obtain a pulse width of about 200 ns, the inductance of a single section of  $LC$  should be in tens of nH, which was impossible for ordinary connection wire. Finally, copper strips were chosen for the PFN, as shown in Fig. 8, and the length of the copper strip in a single section was  $l$ .

TABLE I. Electromagnetic parameters of the PFN-Marx.

$L_1, L_3, L_5$	$L_2, L_4, L_6$	$L_7$	$L_{10}, L_{11}, L_{12}, L_{20}, L_{21}, L_{22}, L_{30}$
100 nH	25 nH	400 nH	100 $\mu$ H



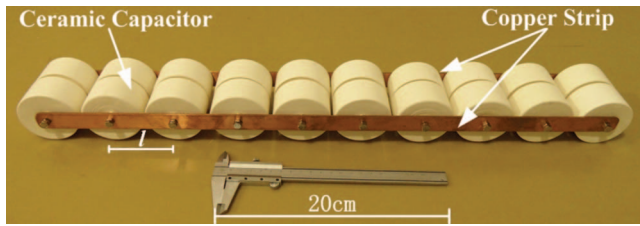


FIG. 8. A single stage PFN with 10 sections of  $LC$  units. (The capacitance of a single ceramic capacitor was 2 nF, and the copper strip was used as connection wire between capacitors.)

As for the copper strip with a rectangular cross-section, the inductance  $L$  can be calculated as follows:<sup>23,24</sup>

$$L = 0.2l \left( \ln \frac{2l}{b+c} + 0.5 + 0.2235 \times \frac{b+c}{l} \right), \quad (3)$$

where  $l$  is the length of the copper strip;  $b$  and  $c$  are the width and length of the cross-section, respectively;  $l$ ,  $b$ , and  $c$  are in unit of mm, and the unit of  $L$  is nH. With parameters of  $l = 66$  mm,  $b = 2$  mm, and  $c = 20$  mm, the inductance  $L$  was calculated as 31 nH. The total inductance of a single  $LC$  section was 62 nH, and the capacitance was 1 nF. The impedance of a single stage PFN was calculated as 8  $\Omega$ , the matched impedance of the 6-stage PFN-Marx was 48  $\Omega$ .

## B. Two sets of pulse transformers and switch unit

The positive charging voltage and the negative charging voltage were controlled by two different pulse transformers. We had to ensure that the two pulse transformers had the



FIG. 9. Two sets of pulse transformers controlled by thyristors. (Thyristors were used as primary switch in the transformer primary loop.)

same parameters and discharged to the PFNs at the same time. Then, two sets of pulse transformers controlled by thyristor were developed, as shown in Fig. 9.

A thyristor is a solid-state semiconductor device that conducts when its gate receives a current trigger and continues to conduct while the current through it is forward biased. One of the advantages of the thyristor as primary switch is that it could transmit high-voltage direct current immediately under an external triggering voltage pulse. The charging time of the pulse transformer was almost 20  $\mu$ s, and the conducting time difference between two thyristors was less than 1  $\mu$ s. Using a single trigger signal, it could be assumed that the two transformers began to charge to their respective secondary capacitors at the same time, and the delay time between two pulse transformers could be neglected.

The switch unit can be seen as Fig. 10, and all the switches were self-fired gas gap switches. The electrode material was copper. The distance between the cathode and anode was adjusted by the polymer gaskets on the cathode. The breakdown voltage of the switches could also be adjusted by filling insulation gases, such as nitrogen, into the unit through the gas-guide tube.

## C. The PFN-Marx system

The high-voltage PFN-Marx generator consisted of two sets of pulse transformers, 6 stages of PFNs with ceramic capacitors, a switch unit, and a match load. The connection circuit was shown as Fig. 3. The pulse transformers and the switch unit were shown as Figs. 9 and 10. The photograph of 6-stage PFN-Marx was shown as Fig. 11, but the isolating inductors were not shown.

The PFNs were placed in three layers and every layer consisted of a pair of PFNs (such as PFN C1 and PFN C2). Here, PFNs A1, B1, and C1 were charged with a positive high-voltage pulse, and PFNs A2, B2, and C2 were charged with negative high-voltage pulse. In order to reduce the inductance in the system, thin copper strips were used as the connection wires between the PFNs and the switch unit.

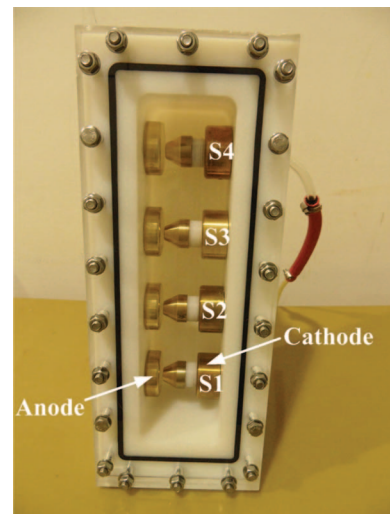


FIG. 10. Switch unit with four self-fired gas gap switches S1 to S4.

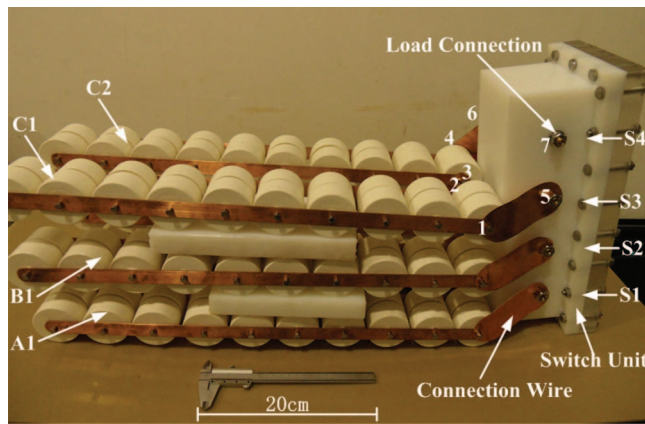


FIG. 11. Photograph of 6-stage bipolar PFN-Marx. (The photograph mainly involved the connection of the 6 stages of PFNs and the switch unit. Thin copper strips were used as the connection wires between the PFNs and the switch unit. Node 1 to node 7 were the connection points. The load connection was connected to the resistor load.)

As shown in Fig. 11, node 1 and node 2 were the two connection ports of PFN C1, and node 3 and node 4 were the connection ports of PFN C2. Node 5 was the anode of switch S3, and node 7 and node 6 was the anode and cathode of switch S4, respectively. The node 1 of PFN C1 was the positive high-voltage port, and the node 4 of PFN C2 was the negative high-voltage port. The connection of the top layer was as follows: node 1 of PFN C1 was connected with the anode of switch S3 (node 5) by a thin copper strip, and PFN C1 and C2 were connected by the copper strip between node 2 and node 3. The other port of PFN C2 (node 4) was connected to the cathode of switch S4 (node 6). The other two layers were connected to switch S1 and switch S2 in a similar fashion. The difference is that the cathode of S1 was connected to the ground. The anode of switch S4 (node 7) was the load connection, which was connected to the resistor load with resistance of  $48\ \Omega$ . Using this design, the volume of the PFN-Marx could be  $80\text{ cm} \times 25\text{ cm} \times 40\text{ cm}$  and the parasitic inductance could be greatly reduced. The PFN-Marx shown in Fig. 11 was placed in transformer oil for insulation during operation.

## V. EXPERIMENTAL RESULTS AND PROMISING APPLICATION

### A. Experimental test of pulse transformer and gas switch

At first, experiments for testing the performance of pulse transformer and gas switch were carried out, and the schematic of the test system was shown as Fig. 12. The relative parameters of the transformer were as follows: the primary and secondary capacitance is  $940\ \mu\text{F}$  and  $33\text{ nF}$ , respectively, and the turns ratio of the primary and secondary winding is 2:270. The maximum voltage across secondary capacitor can be as high as 100 kV and the step-up ratio could reach 160. The protective resistor  $R_1$  was connected with the gas gap switch in series and the switch was surrounded by nitrogen. When the voltage across switch S reached the max-

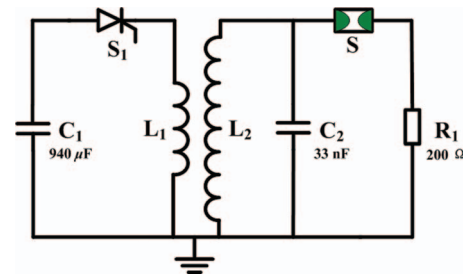


FIG. 12. Schematic of system for the test of pulse transformer and gas switch ( $C_1$  was the primary capacitor and  $C_2$  was the secondary capacitor.  $S_1$  was thyristor in the primary loop, S was gas switch, and  $R_1$  was the protective resistor. The gas switch was surrounded by nitrogen.)

imum voltage that it could sustain, the capacitor  $C_2$  rapidly discharged through the protective resistor  $R_1$ . The peak voltage could be seen as the breakdown voltage across the switch.

By measuring the voltage waveform on capacitor  $C_2$ , the breakdown strength of switch S could be obtained. A typical waveform on capacitor  $C_2$  was shown as Fig. 13. The charging time was about  $20\ \mu\text{s}$  and the peak voltage was 85 kV here. Usually, the breakdown voltage depended on the electrode space  $d$  between the anode and cathode and the pressure of nitrogen in it.

The average breakdown voltage of switch with different electrode spaces and gas pressures was shown as Fig. 14. Here, each average breakdown voltage was the statistical result of more than 20 times of individual breakdown process. According to Fig. 14, the average breakdown voltage was almost linear to the gas pressure and it was increased with the increasing of electrode space. Besides, when the space was 2 mm, the average breakdown voltage was about 20 kV, which was much lower than the breakdown voltage with other electrode spaces.

The coefficient of variance (CV) was used to describe the discrete level of breakdown voltage here, and the CV for breakdown voltage was shown in Fig. 15. It can be seen that the CV for breakdown voltage was greatly decreased with the increasing of gas pressure. The CV was more than 10% at standard atmospheric pressure, while it could be reduced to lower than 5% at 3 atms, which indicated that a higher gas

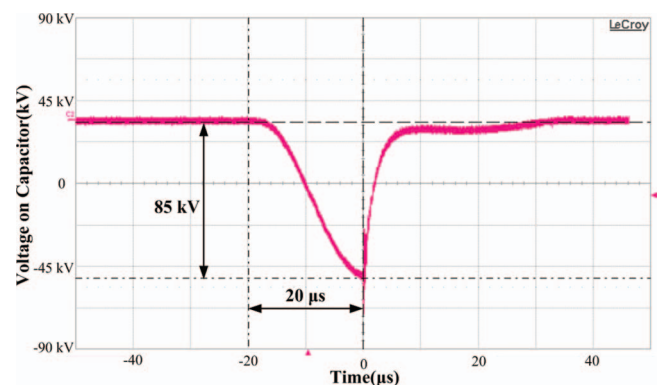


FIG. 13. Typical voltage waveform on the secondary capacitor  $C_2$ . (The charging voltage on the primary capacitor was 530 V.)

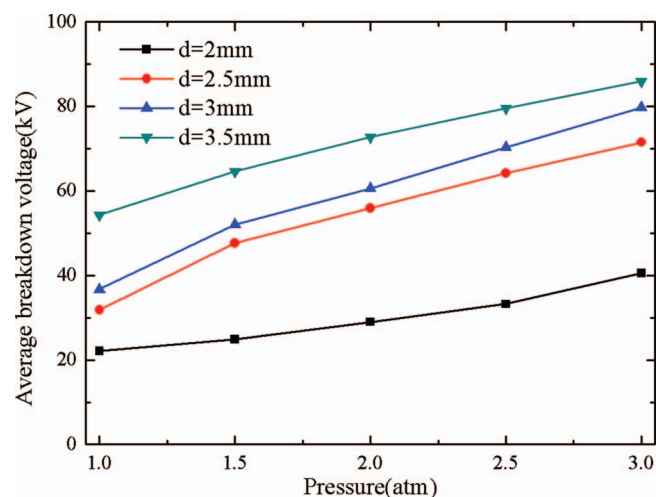


FIG. 14. Average breakdown voltage of switch under different electrode spaces and gas pressures.

pressure and over-voltage could reduce the jitter of the gas switch.

## B. PFN-Marx system tests

Next, the performance of a single stage PFN was tested by experiments. The output voltage signals were measured by a resistive voltage divider, and the resistive divider could respond well to ns-range pulses. Output voltage of single stage PFN was shown in Fig. 16. The charging voltage on a single stage PFN was 75 kV and the load resistance is 8  $\Omega$ . It can be seen that the pulse width of the output pulse was about 170 ns and the voltage amplitude could be calculated as 36 kV. The experimental result was consistent with the theoretical calculation result by Eq. (1), where the pulse width of a single stage was calculated as about 160 ns.

Finally, experiments were carried out to demonstrate the feasibility of the PFN-Marx system. The output voltage pulse of 6-stage bipolar PFN-Marx gained on the matching resistive load of 48  $\Omega$  was shown in Fig. 17. The charging volt-

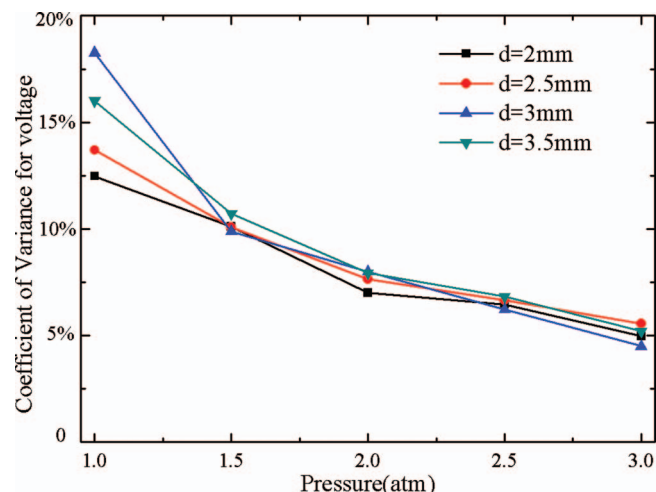


FIG. 15. The coefficient of variance (CV) for breakdown voltage under different electrode spaces and gas pressures.

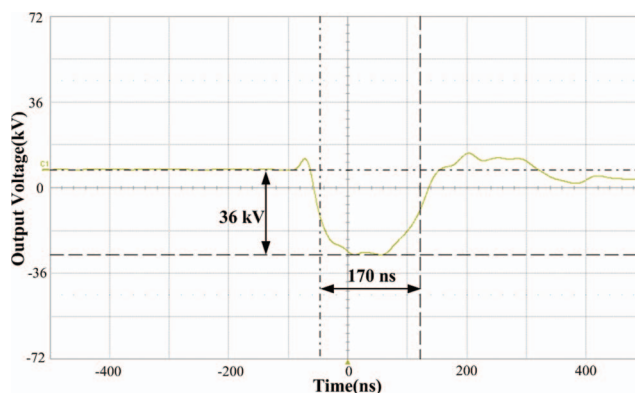


FIG. 16. Output voltage of a single stage PFN vs. discharge time. (The charging voltage on the single PFN was 75 kV and the load resistance was 8  $\Omega$ .)

age waveform was similar to the waveform in Fig. 13 and the peak voltage on the PFNs was 35 kV. According to Fig. 17, the pulse width was 173 ns and the rise time was less than 15 ns. The voltage amplitude of the output pulse was 100 kV and the step-up ratio was 2.86. It can also be found that the flat top and the tail of the pulse were not perfected and the pulse had an oscillation there. We suppose that the phenomenon was caused by the mismatching of the water resistor load. It is known that the resistance of water resistor was greatly depended on temperature and a high-voltage pulse may change the temperature on the load.<sup>25</sup> Other parameters, such as parasitic inductance and resistance, in the measuring circuit could have also affected the testing results.

## C. Promising application

Our target was to produce a solid-state, compact, high-voltage, long pulse generator. The parameters of the PFN determined the waveform of the pulse and the Marx generator achieved the multiplication of voltage. There were 6 stages of PFNs in the system and the output voltage would be higher with more PFNs stages. If the self-fired switch used in the first stage was replaced by a triggered switch, the jitter of the switches would be reduced and repetition rates could be achieved.

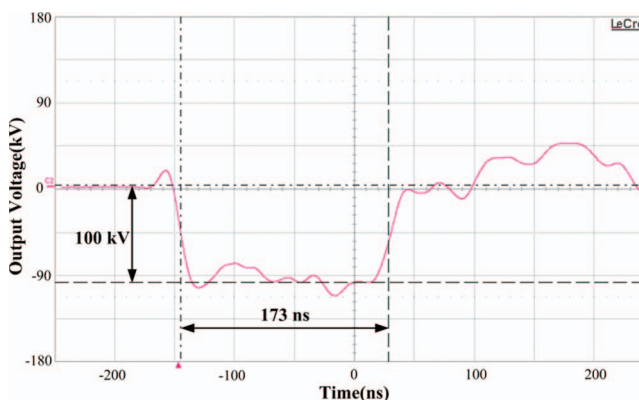


FIG. 17. Output voltage waveform of 6-stage bipolar PFN-Marx on the load vs. discharge time. (The charging voltage on the every PFN was 35 kV and the load resistance was 48  $\Omega$ .)



One industrial application of the PFN-Marx generator would be to investigate pulsed electrical breakdown phenomena, which has been applied to many fields including high-voltage switching, high-voltage insulation, and energy storage.<sup>26</sup>

For example, due to the characteristics of high breakdown strength, transformer oil was usually utilized as insulation dielectric in the high-voltage system. The dielectric strength of transformer oil using microsecond and sub-microsecond voltage pulses has already been experimentally studied. The breakdown strength of a dielectric can be different under high-voltage pulses with widths of microseconds and nanoseconds. The rise time could also affect the breakdown strength. Using this system, the electrical breakdown and recovery characteristics of dielectric, such as transformer oil and other energy storage dielectrics, under high-voltage pulses with widths of about 200 ns could be obtained.

Another promising application was for material processing,<sup>26,27</sup> such as material ablation, surface heating, and surface processing. For example, the sample would be fixed between the anode and cathode of the generator and the intense electron beams would be extracted from the cathode during operation. The beams would strike at the surface of the sample and the energy spectrums and other relative parameters could be used to obtain the properties the material.

## VI. CONCLUSIONS

The PFN-Marx generator was an effective way to generate a high-voltage square pulse. In this paper, the discharge characteristic of a single stage PFN was discussed. The charging and discharge processes of the PFN-Marx were simulated by PSpice software. It was found that, compared with isolating inductors connected in series type, the over-voltage on the switches was much larger with isolating inductors in parallel type connection. Additionally, the bipolar charging scheme could also reduce the number of switches. All of these were helpful to reduce the jitter of the switches. The structure of the PFN-Marx system was designed to be compact to decrease the parasitic inductance. Ceramic capacitors with high relative permittivity and withstand voltage were employed as the storage capacitors in the PFN. With the multiplication of voltage in Marx type configuration, the output voltage had been improved greatly. According to the circuit simulations and the structure design, a compact 6-stage bipolar PFN-Marx based on pulse transformer was constructed. The output voltage on the matching resistive load of 48  $\Omega$  was 100 kV with a pulse width of 173 ns and rise time less than 15 ns.

## ACKNOWLEDGMENTS

The authors wish to thank X. Zhou and J. C. Wen for their encouragement and valuable suggestion. The assistance of Y. Q. Tang in the experiment is also gratefully acknowledged. This work is supported by the Fund of Innovation, Graduate School of National University of Defense Technology (S130703).

- <sup>1</sup>G. A. Mesyats, S. D. Korovin, V. V. Rostov, V. G. Shpak, and M. I. Yalandin, *Proc. IEEE* **92**(7), 1166–1179 (2004).
- <sup>2</sup>A. V. Gunin, A. I. Klimov, S. D. Korovin, and I. V. Pegel, *IEEE Trans. Plasma Sci.* **26**(3), 326–331 (1998).
- <sup>3</sup>J. C. Su, X. B. Zhang, G. Z. Liu, X. X. Song, and Y. F. Pan, *IEEE Trans. Plasma Sci.* **37**(10), 1954–1958 (2009).
- <sup>4</sup>G. A. Mesyats and S. D. Korovin, *Laser Part. Beams* **21**(2), 197–209 (2003).
- <sup>5</sup>J. L. Liu, Y. Yin, and B. Ge, *Rev. Sci. Instrum.* **78**, 103302 (2007).
- <sup>6</sup>J. L. Liu, C. L. Li, and J. D. Zhang, *Laser Part. Beams* **24**(3), 355–358 (2006).
- <sup>7</sup>Y. Zhang, J. L. Liu, X. B. Cheng, G. Q. Bai, H. B. Zhang, and J. H. Feng, *Rev. Sci. Instrum.* **81**, 033302 (2010).
- <sup>8</sup>Y. Zhang, J. L. Liu, X. B. Cheng, H. B. Zhang, and G. Q. Bai, *IEEE Trans. Plasma Sci.* **38**(4), 1019–1027 (2010).
- <sup>9</sup>S. D. Korovin, V. P. Gubanov, A. V. Gunin, I. V. Pegel, and A. S. Stepchenko, 28th IEEE International Conference on Plasma Science, Las Vegas, **2**, 1249–1251 (2001).
- <sup>10</sup>S. Friedman, R. Limpacher, and M. Sirchis, *IEEE Power Modulator Symp.* **1**, 360–366 (1988).
- <sup>11</sup>M. M. Kekez, *Pulsed Power Plasma Sci.* **2**, 1027–1030 (2001).
- <sup>12</sup>J. Hammon, S. K. Lam, and S. Pomemy, *IEEE Pulse Power Conf.* **1**, 429–434 (1995).
- <sup>13</sup>M. M. Kekez, *IEEE Pulse Power Conf.* **2**, 1524–1529 (1997).
- <sup>14</sup>D. A. Phelps, *IEEE Power Modulator Symp.* **1**, 507–510 (1990).
- <sup>15</sup>J. Hammon, S. K. Lam, and D. Drury, *IEEE Pulse Power Conf.* **1**, 147–152 (1997).
- <sup>16</sup>H. T. Li, H.-J. Ryoo, and J.-S. Kim, *IEEE Trans. Plasma Sci.* **37**(1), 190–194 (2009).
- <sup>17</sup>X. L. Fan and J. L. Liu, *Rev. Sci. Instrum.* **84**, 064703 (2013).
- <sup>18</sup>H. X. Xiao, L. Li, H. F. Ding, T. Peng, and Y. Pan, *IEEE Trans. Power Electron.* **26**(12), 3817–3822 (2011).
- <sup>19</sup>R. M. Ness, B. D. Smith, E. Y. Chu, B. L. Thomas, and J. R. Copper, *IEEE Trans. Electron Devices* **38**(4), 803–809 (1991).
- <sup>20</sup>J. C. Zheng, L. D. Xie, Y. M. Zhao, L. M. Wang, and Z. C. Guan, *IEEE Trans. Dielectr. Electr. Insul.* **19**(4), 1369–1376 (2012).
- <sup>21</sup>M. T. Domonkos, S. Heidger, D. Brown, J. V. Parker, and C. W. Gregg, *IEEE Trans. Plasma Sci.* **38**(10), 2686–2693 (2010).
- <sup>22</sup>M. J. Pan and C. A. Randall, *IEEE Electr. Insul. Mag. (USA)* **26**(3), 44–50 (2010).
- <sup>23</sup>H. Hertwig, *Induction calculation* (National Defense Industry Press, Beijing, 1960) (in Chinese).
- <sup>24</sup>Q. F. Wang, G. Q. Gao, Q. X. Liu, Z. Q. Zhang, and K. S. Hu, *High Power Laser Part. Beams* **21**(4), 531–535 (2009).
- <sup>25</sup>W. Jia, W. Q. Chen, C. G. Mao, and J. T. Zeng, *Rev. Sci. Instrum.* **81**, 034703 (2010).
- <sup>26</sup>H. Akiyama, T. Sakugawa, and T. Namihira, *IEEE Trans. Dielectr. Electr. Insul.* **14**(5), 1051–1064 (2007).
- <sup>27</sup>Y. Zhang, J. L. Liu, X. L. Fan, H. B. Zhang, and S. W. Wang, *Rev. Sci. Instrum.* **82**, 104701 (2011).